

A laser desorption ionisation mass spectrometry approach for high throughput metabolomics

Seetharaman Vaidyanathan^a, Dan Jones^b, David I. Broadhurst^a, Joanne Ellis^a, Tudor Jenkins^b, Warwick B. Dunn^a, Andrew Hayes^c, Nicola Burton^c, Stephen G. Oliver^c, Douglas B. Kell^a, and Royston Goodacre^{a,*}

^aSchool of Chemistry, The University of Manchester, PO Box 88 Sackville Street, Manchester, M60 1QD, UK

^bInstitute of Mathematical and Physical Sciences, University of Wales, Aberystwyth, Wales, UK

^cFaculty of Life Sciences, The University of Manchester, Michael Smith Building, Oxford Road, Manchester, M13 9PT, UK

Received 24 May 2005; accepted 13 June 2005

The importance of metabolomic data in functional genomic investigations is increasingly becoming evident, as is its utility in novel biomarker discovery. We demonstrate a simple approach to the screening of metabolic information that we believe will be valuable in generating metabolomic data. Laser desorption ionisation mass spectrometry on porous silicon was effective in detecting 22 of 30 metabolites in a mixture in the negative-ion mode and 19 of 30 metabolites in the positive-ion mode, without the employment of any prior analyte separation steps. Overall, 26 of the 30 metabolites could be covered between the positive and negative-ion modes. Although the response for the metabolites at a given concentration differed, it was possible to generate direct quantitative information for a given analyte in the mixture. This technique was subsequently used to generate metabolic footprints from cell-free supernatants and, when combined with chemometric analysis, enabled us to discriminate haploid yeast single-gene deletants (mutants). In particular, the metabolic footprint of a deletion mutant in a gene encoding a transcriptional activator (Gln3p) showed increased levels of peaks, including one corresponding to glutamate, compared to the other mutants and the wild-type strain tested, enabling its discrimination based on metabolic information.

KEY WORDS: Laser desorption ionisation; high-throughput metabolomics; metabolic footprinting; yeast; functional genomics.

1. Introduction

Saccharomyces cerevisiae is among the most well-studied organisms of the post-genome era. However, even for such an important model eukaryote over 2000 ORFs (about 30% of protein-encoding genes in its genome) remain poorly characterised (<http://www.yeastgenome.org/>); that is to say there is no unequivocal knowledge about the genes' role. Whilst functional genomic investigations involving transcriptomic and proteomic analyses are being actively pursued to enhance our understanding of gene functions (e.g., Bader *et al.*, 2003; Jones *et al.*, 2003; Vazquez *et al.*, 2003; Wu *et al.*, 2004), there is more to gain from examining the metabolomes that can provide valuable additional information (Castrillo and Oliver, in press; Oliver *et al.*, 1998; Raamsdonk *et al.*, 2001; Vaidyanathan, 2005; Vaidyanathan *et al.*, 2005). This is highlighted by the significant role metabolites play in the regulation of gene function, several of which can go unnoticed when transcriptomes and proteomes alone are

analysed (Daran-Lapujade *et al.*, 2004; Ideker *et al.*, 2001; ter Kuile and Westerhoff, 2001). There is thus considerable interest in developing strategies for analysing metabolomes, of which metabolic footprinting shows promise for rapid and high-throughput screening and analysis (Allen *et al.*, 2003, 2004; Kaderbhai *et al.*, 2003; Kell *et al.*, in press).

Metabolites secreted into the culture medium, as a result of "overflow metabolism," can provide valuable information on microbial behaviour, in addition to that from intracellular metabolites, and these "metabolic footprints" can be used for functional genomic investigations (Allen *et al.*, 2003, 2004; Kaderbhai *et al.*, 2003). The main attraction in such analyses is the avoidance of the need to extract metabolites from within cells and the associated discrepancies/difficulties that are involved in the analyses of intracellular metabolites, such as rapid quenching of metabolism and separation from extracellular metabolites. Whilst techniques such as direct-infusion electrospray ionisation mass spectrometry (DI-ESMS), NMR spectroscopy, GC-MS, FT-IR and Raman spectroscopies, can be used for deriving metabolic footprints (Goodacre *et al.*, 2004; Dunn *et al.*, 2005; Dunn and Ellis, 2005), alternative technologies

*To whom correspondence should be addressed.
E-mail: Roy.Goodacre@manchester.ac.uk

that can rapidly generate useful information about metabolite levels with minimal sample intervention would provide a welcome addition to the functional genomics “toolbox.” Such rapid screening methods would be used prior to more elaborate and directed metabolite analyses, as part of a hierarchical approach.

Laser desorption ionisation mass spectrometry on porous silicon (DIOS), pioneered by Siuzdak *et al.* (Wei *et al.*, 1999; Shen *et al.*, 2001; Go *et al.*, 2003a, b; Trauger *et al.*, 2004) has been shown to be a simple and useful method for analysing small molecules without the intervention of matrix ions and adducts typically associated with MALDI-MS analyses. In these investigations the emphasis has been on the analysis of one or two small molecules, usually in isolation. The suitability of the technique for the analysis of mixtures of small molecules (as would be encountered in metabolomic investigations) has, to our knowledge, not been shown. We therefore studied the application of DIOS with cluster analysis for metabolic footprinting, and report here the proof-of-principle of this concept for the discrimination of different yeast single gene deletant (hereafter referred to as mutant) strains.

2. Materials and methods

2.1. Microbial growth

Ten *MATa* haploid *Saccharomyces cerevisiae* mutants and the corresponding wild-type strain (table 1) were grown in batch cultures using a minimal medium as described earlier (Allen *et al.*, 2003). Briefly, ammonium was the main nitrogen source and a cocktail of amino acids consisting of arginine, aspartate, glutamate, histidine, leucine, lysine, methionine, serine, threonine, tryptophan and valine, all at 1 mM concentration, was available for growth. The mutants were grown as three biological replicates. After 24 h of growth (sufficient time for the mutants to have entered the stationary phase of growth [Allen *et al.*, 2003]), the cells were

centrifuged and the cell-free broth was collected and stored at -80°C until analysed.

2.2. Metabolite cocktail

This consisted of the amino acids (in L-form) alanine, arginine, asparagine, cysteine, glutamine, glycine, histidine, isoleucine, leucine, lysine, methionine, phenylalanine, proline, serine, threonine, valine (all at $30\ \mu\text{M}$), aspartate, glutamate, tryptophan (all at $3\ \mu\text{M}$), tyrosine ($0.3\ \mu\text{M}$), the organic acids fumarate ($3\ \mu\text{M}$), citrate, malate, lactate, pyruvate, succinate, oxaloacetate (all at $30\ \mu\text{M}$), and the metabolites 4-aminobutyric acid, putrescine and D-glucose (all at $30\ \mu\text{M}$).

2.3. Mass spectrometry

Frozen, cell-free supernatants were thawed and diluted 1 in 10 using deionised water. The diluted samples were spotted directly on to a DIOS porous silicon target chip (Mass Consortium Inc., San Diego, CA, USA). The DIOS chip was then attached to a standard stainless steel target plate using double sided sticky conductive carbon tape (Structure Probes Inc., West Chester, PA, USA) and analysed in a Kratos Axima CFR + MALDI-ToF mass spectrometer (Kratos Analytical, Manchester, UK), in both the positive and negative-ion modes. 150 shots were averaged for each sample in both the acquisitions, and typical spectral collection times were 2 min per sample. Each biological replicate was analysed four times (technical replicates). The DIOS chip was washed with methanol several times (typically five) and reused where required, for replicate analyses.

2.4. Data analysis

The mass spectral data were imported into MATLAB (The Math Works, Natick, MA, USA) and processed for analysis as described (Goodacre *et al.*, 1998; Raamsdonk *et al.*, 2001). The spectra (in the mass range

Table 1
The *MATa* haploid mutants used in the study and their physiological significance

Mutant ORF	Description (/mutation in)	Identifier
BY4741	Wild type strain (<i>MATa</i> ; <i>his3Δ1</i> ; <i>leu2Δ0</i> ; <i>met15Δ0</i> ; <i>ura3Δ0</i>)	wh
YDR508c (<i>gnp1Δ</i>)	Broad-specificity amino-acid permease. High-affinity glutamine permease	s1
YBR294w (<i>su1Δ</i>)	Sulfate permease I	s2
YCR037c (<i>pho87Δ</i>)	Low affinity phosphate transporter	s3
YPR138c (<i>mep3Δ</i>)	Low affinity ammonium permease	s4
YKL040c (<i>nfu1Δ</i>)	Iron homeostasis	c1
YCR044c (<i>per1Δ</i>)	Involved in manganese homeostasis	c2
YAL062w (<i>gdh3Δ</i>)	NADP-glutamate dehydrogenase	c3
YER040w (<i>gln3Δ</i>)	Transcription factor for positive nitrogen regulation. Responsible for nitrogen catabolite repression (NCR)-sensitive transcription.	g1
YKR034w (<i>dal80Δ</i>)	Transcriptional repressor for allantoin and GABA catabolic genes. Negative regulator of multiple nitrogen catabolic genes	g2
YLR013w (<i>gat3Δ</i>)	Transcription factor activity. Similarity to nitrogen regulatory proteins	g3

100–500 m/z) were binned to 0.1, 0.2 or 0.5 m/z and normalised to total ion counts. Principal components analysis (PCA) was performed using the NIPALS algorithm and a selected number of PCs (typically those contributing to more than 95% of the explained variance) chosen for discriminant function analysis (DFA), where the mutant type was used as the *a priori* known class information. Clustering on the PC-DFA space was then studied. Reproducibility was assessed by choosing one of the biological replicates for each mutant class as the test set and retaining the other two biological replicates in the training set.

3. Results and discussion

DIOS spectra of a cocktail of 30 metabolites consisting of 20 amino acids and a few (5) organic acids showed spectral information pertaining to the metabo-

lites in the protonated $[M+H]^+$, sodiated $[M+Na]^+$ or potassiated $[M+K]^+$ forms in the positive-ion mode (figure 1a) or the deprotonated form $[M-H]^-$ in the negative-ion mode (figure 1b). As expected, the basic metabolites (arginine, histidine, putrescine) dominated the positive-ion spectra, whilst the acidic ones (malic acid, citric acid) dominated the negative-ion spectra. When the metabolites were analysed in isolation, at an equimolar concentration of 30 μM , the response of the individual metabolites was different from each other, as illustrated for analysis in the negative-ion mode, in figure 1c. Cysteine, glucose, oxaloacetate, putrescine and succinate did not show detectable signals. Differences in the response could be observed for metabolites with identical or near identical mass, so that it is possible in favourable cases, to assign signals from mixtures to one or the other metabolite. The deprotonated forms of oxaloacetate and asparagine are expected to have a

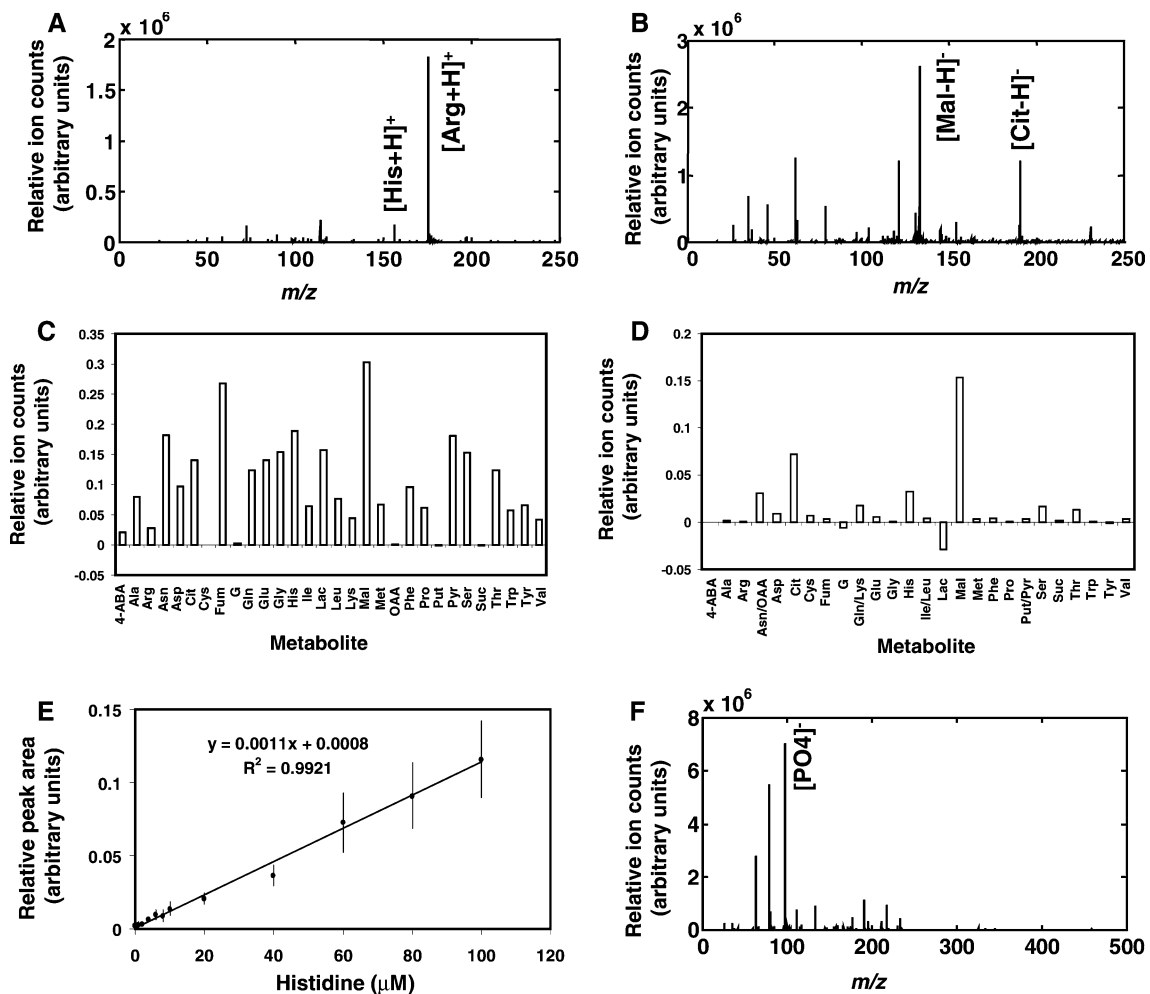


Figure 1. Desorption ionisation mass spectra on porous silicon of a metabolite cocktail containing 30 standard metabolites (refer to text for details) in (a) the positive-ion mode and (b) the negative-ion mode; (c) Relative median metabolite response for each of the thirty metabolites when analysed individually at 30 μM concentration, in the negative-ion mode; (d) The observed relative median response in the negative-ion mode, corresponding to each metabolite in the cocktail when the mixture was analysed; (e) Quantitative information (calibration curve) in the positive-ion mode for histidine obtained by spiking a metabolic cocktail containing the twenty amino acids minus histidine (at 50 μM each), with histidine at concentrations of 0–100 μM and monitoring peak areas relative to TIC (error bars indicate 1 standard deviation either side of the mean); (f) Average negative-ion spectra of cell free supernatant from the culture of a mutant (g1) after 24 h of growth. Note the prominent phosphate peak which was removed when these data were analysed by clustering algorithms.

signal at m/z 131.1 in the negative-ion mode. Whilst asparagine shows a detectable response at this m/z , oxaloacetate was not detectable. A detectable response at this m/z in a mixture containing both species can thus be assigned to asparagine. Similarly, glutamine gives a better response than does lysine at m/z 145.1, and the response at this m/z in a mixture containing both can be expected to have a greater contribution from glutamine. However, for leucine and isoleucine, both of which are expected to give a response at m/z 130.2 in the negative-ion mode, the difference is marginal, making it difficult to assign contributions directly.

The median response of the metabolites when analysed in a mixture showed 22 detectable signals at the expected m/z corresponding to the 30 metabolites in the negative-ion mode (figure 1d). Tyrosine, fumarate, glutamate, aspartate and tryptophan were present at lower concentration than the rest, and consequently showed lower signal responses. The presence of other metabolites appears to influence the detection of a response to a particular metabolite, as well as the concentration of the metabolite in the mixture, as almost all the signals were lower than expected. In the positive ion mode, signals at m/z corresponding to 19 of the 30 metabolites in the mixture could be detected. Signals at m/z corresponding to metabolites like succinate, lactate and glucose in the mixture, which gave little or no signal in the negative-ion mode could be detected as sodium or potassium adducts in the positive-ion mode, albeit with a weak signal. Overall, excluding four of the metabolites that had the same nominal mass as four others, signals corresponding to all the other metabolites (26 in number) could be detected in the positive or the negative ion mode, at varying levels of signal intensity.

Although the responses differed for each metabolite, the peak areas normalised to the total ion current (TIC) varied in proportion to the concentration of the metabolite, even in a mixture, as demonstrated in figure 1e for histidine, when varying concentrations of histidine were spiked in a metabolic cocktail containing 19 of the 20 amino acids in the mixture (histidine was omitted). Varying the concentration of histidine resulted in a proportional change in the normalised peak area at m/z 156.2, where the protonated histidine gives a signal in the positive-ion mode. It was possible to detect a proportional response for histidine from 1 μM to 1 mM, with linear responses over different concentration ranges. The calibration curve obtained in the concentration range 0–100 μM is shown in figure 1f. This demonstrates clearly that, in addition to detecting spectral signals, it is also possible to obtain quantitative information using this technique.

In order to assess the suitability of this technique for metabolomics studies, we investigated the classification of yeast mutants based on their metabolic footprints. We selected 10 *MATa* haploid mutants (table 1) of *S. cerevisiae*, derived from the wild type strain BY4741.

Three of these (c1–c3) are associated with the central metabolic pathways and/or in maintaining homeostasis, three others (g1–g3) are associated with the regulation of gene expression (influencing activity of transcription factors), and the rest (s1–s4) are associated with external sensing/transport and/or signal transduction. The strains were cultivated to the stationary phase of growth, as this had been shown previously to give the most reproducible metabolic footprint (Allen *et al.*, 2003). The cell free supernatants were then harvested and their dilutions analysed using DIOS-MS in both the positive- and negative-ion modes, without any prior analyte separation stages (such as chromatography).

Much of the spectral information in the positive-ion mode appeared to be suppressed with dominant K^+ and Na^+ ions, possibly due to the high salt concentrations in the growth medium. However, the negative-ion spectra showed peaks that corresponded to organic acids of primary metabolism, some of which were components of the growth medium. A typical spectrum (average of replicate measurements) in the negative-ion mode (figure 1f) is dominated by a signal at m/z 97 that corresponds to phosphate in the growth medium (this signal completely suppresses other signals in negative-ion DIOSMS). To minimise this dominant influence the spectra were analysed from m/z 100 to m/z 500. After spectral preprocessing the dimensionality of the data was reduced by PCA to extract the predominant variance and the first few PCs that contributed to over 95% of the variance analysed by DFA to obtain discriminant information.

Figure 2a shows a pseudo 2D scores plot of the samples for the first two discriminant functions (first 60 PCs used for DFA), and it can be seen that the mutant labeled g1 clearly separates out from the rest of the yeast strains including the wild type. Although the *a priori* information used in the clustering is the mutant classification itself, the reproducibility of the discrimination can be observed by the clustering of the test set (labeled with an asterisk) along with the training set. An inspection of the first combined PC-DFA loadings (figure 2b) demonstrates that the major variations modeled are based on the changes in m/z 145.1 and 146.1. These mass units correspond to those of the deprotonated forms of the amino acids glutamine (and/or lysine, α -ketoglutarate) and glutamate, respectively. A comparison of the mean spectra of the g1, g2 and the wild-type strains shows clearly the difference between the strains in peak at m/z 146 attributable to glutamate (figure 2c), and in particular that this peak is more intense in g1 compared to the rest. These results are corroborated by observations from DIOSMS of the samples in the positive-ion mode (figure 2d), where glutamate and glutamine peaks showed a higher response for g1, compared with g2 and the wild type. Similarly, it was also observed from GC-MS analysis of the mutants (data not shown) that the mean peak area corresponding to glutamate for

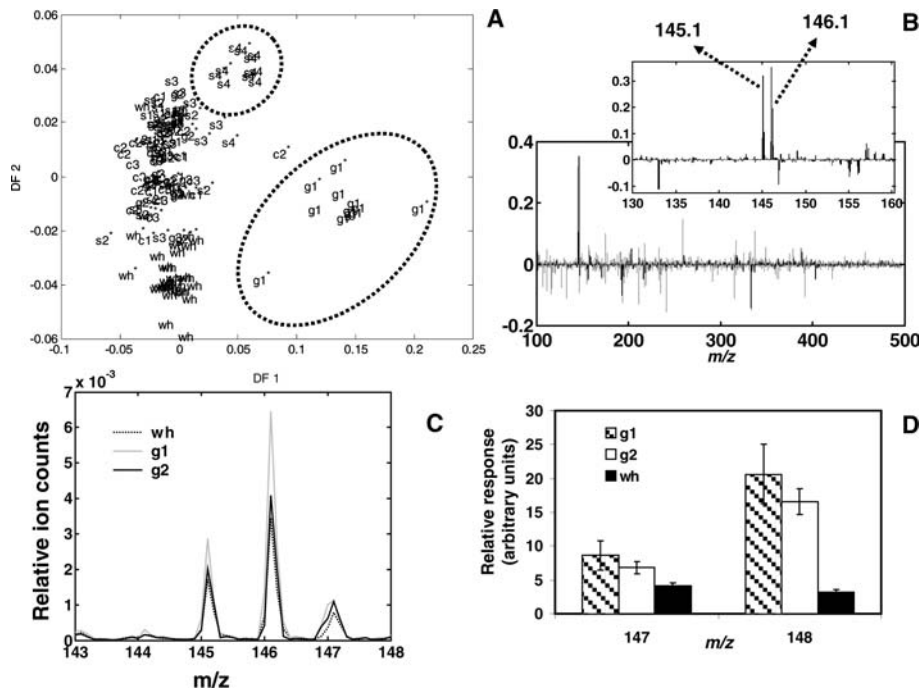


Figure 2. (a) PC-DFA score plot constructed using the first 60 PCs (analysed on spectra binned to 0.1 m/z) showing the discrimination of mutants g1 and s4 from the rest of the yeast mutants and the wild type strain. The test set is marked with an asterisk, and the separating clusters encircled for clarification. (b) The first loadings plot of the PC-DFA. Note the prominent peaks at m/z 145 and 146 seen clearly in the expanded portion of the loadings. (c) Mean spectra of g1 (*gln3* Δ), g2 (*dal80* Δ) and the wild type wh (BY4741) strains showing the differences in the spectra in the region where the prominent discriminatory effect is observed. Note the higher peak intensity at m/z 146 (corresponding to glutamate) for g1 compared to the rest. (d) Mean spectral response corresponding to glutamine (m/z 147) and glutamate (m/z 148) in the positive-ion direct infusion electrospray ionisation mass spectra of the three strains as in (c) (error bars represent one standard deviation about the mean).

the metabolic footprint of g1 mutant was higher than that of g2 or the wild type.

From table 1, the mutant g1 can be identified as YER040w which is a single deletion mutant in *GLN3*, which encodes a transcriptional activator of genes regulated by nitrogen catabolite repression that is, itself, regulated by the type of the nitrogen source available for use.

The product of *GLN3* is under the control of the TOR signaling pathway, which mediates the cell's response to nutrient supply, and is a key element in the regulation of the expression of a number of genes in *S. cerevisiae* in response to the availability of different sources of nitrogen (Mitchell and Magasanik, 1984; Beck and Hall, 1999; Cooper, 2002). The TOR cascade has a prominent role in regulating translation, ribosome biogenesis and amino-acid permease stability, in addition to transcriptional regulation (Cardenas *et al.*, 1999; Kuruvilla *et al.*, 2001). The *GLN3* regulatory system responds to intracellular glutamine levels (Mitchell and Magasanik, 1984; Crespo *et al.*, 2002), and is activated under nitrogen-limiting conditions or when a poor nitrogen source is available.

In yeast, the quality of the available nitrogen source controls the expression of genes encoding proteins responsible for the uptake and assimilation of nitrogenous compounds (Kuruvilla *et al.*, 2001; Magasanik and Kaiser, 2002). Four GATA transcription factors, the activators Gln3p and Gat1p/Nil1p and the repressors

Dal80p and Deh1p/Nil2p/Gzf3p mediate the regulation of this process (Cooper, 2002). In the presence of a good source of nitrogen, such as glutamine or ammonium, the *GLN3* product Gln3p is retained in the cytoplasm in a phosphorylated form bound to Ure2p, and is inactive. Upon a shift to a nitrogen-poor environment or in the presence of poor nitrogen sources such as proline, urea or glutamate, Gln3p is dephosphorylated, dissociated from Ure2p, and enters the nucleus to promote transcription of the genes needed for the transport and catabolism of the available poor nitrogen source. Gln3p activates genes encoding glutamine synthetase, glutamate synthase, glutamate dehydrogenase (all enzymes involved in nitrogen source metabolism), in addition to those encoding the GATA activator, Gat1p/Nil1p and the repressor, Dal80p (Daugherty *et al.*, 1993; Magasanik and Kaiser, 2002). It thus plays a crucial role in the regulatory mechanism under nitrogen limiting conditions. Deletion mutants of *GLN3* show poor activities of some of the above enzymes (Mitchell and Magasanik, 1984; Courchesne and Magasanik, 1988) in the presence of glutamate. Under the culture conditions employed in our study, after the depletion of ammonium (the primary nitrogen source) the utilisation of secondary nitrogen sources (such as glutamate) would be hampered in the *gln3* deletion mutant, leaving some of these sources unused in the medium. Alternatively, the metabolites detected in the medium that contribute to

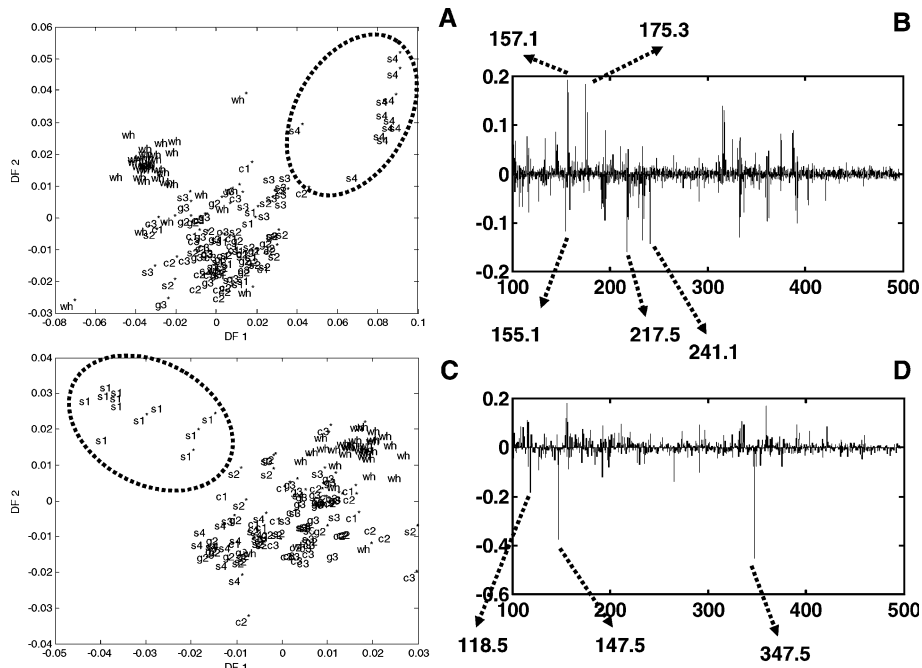


Figure 3. Discrimination of mutants after excluding *g1* spectra from the analysis (a) PC-DFA score plot of analysis performed on spectra binned to 0.1 m/z , constructed using the first 65 PCs, showing the discrimination of mutant *s4*. (b) The first PC-DFA loadings plot showing the regions of major variance in the spectral data, corresponding to the analysis in (a). (c) PC-DFA score plot of analysis done on spectra binned to 0.5 m/z , showing the discrimination of mutant *s1*. (d) The first PC-DFA loadings plot showing the regions of major variance in the spectral data corresponding to the analysis in (c). The test set is marked with an asterisk and the clusters encircled for clarification, in (a) and (c).

the discrimination of these mutants from the rest could have been excreted as a result of improper metabolism. Such excretions are not uncommon in *S. cerevisiae* cultivations (Velasco *et al.*, 2004). Although the physiological reasons for the discrimination are difficult to ascertain within the current experimental setup, the fact that the metabolic footprint of the *gln3* mutant separates from that of the *dal80* mutant (*g2*) which is also associated with regulation of nitrogen metabolism, albeit with a different mechanism (Daugherty *et al.*, 1993; Cooper, 2002), suggests that the technique adopted in this investigation has the ability to discriminate between similar physiological processes and thus is a potentially valuable tool in functional genomic investigations.

Further analysis of the dataset after removal of the *g1* mutant data showed that the mutants *s1* and *s4* can be discriminated based on their metabolic footprints (figure 3). Indeed, *s4* can be seen to cluster separately even when *g1* is included in the analysis (figure 2a), but the discrimination is better following removal of the *g1* DIOS data. Whilst *s4* discrimination is observed only in the analysis of the spectral data with 0.1 m/z resolution (figure 3a), *s1* discrimination is observed when a 0.5 m/z resolution is used (figure 3c). This is possibly due to overlap of spectral information and the difficulty in discriminating between the information due to *s1* in the presence of more data (i.e., the information is possibly lost in the presence of too many peaks). From table 1, these mutants can be identified to be YDR508c and YPR138c. The first mutant is a *gnp1* deletant and thus

lacks a broad-specificity amino acid permease/high-affinity glutamine permease. The second mutant is deleted for *MEP3*, which encodes a low affinity ammonium permease. Inspection of the first loadings plot for these two discriminations (figure 3b, d) shows changes at m/z 118.5, 147.5 and 347.5 contributing most to the discrimination of *s1*, whilst m/z 155.1, 157.1, and 173.3 are among the peaks contributing to the discrimination of *s4*. Although there are several metabolites that could potentially contribute to these masses, two candidates for the mass unit at 118, threonine and/or homoserine have a known physiological significance. It is known that *GNP1* is expressed under both rich and poor nitrogen conditions and cells lacking *GNP1* exhibit reduced levels of glutamine transport (Zhu *et al.*, 1996). *Gnp1p* has also been implicated in threonine and homoserine uptake systems in yeast and excretion of these metabolites into the medium with deletion mutants have been observed (Velasco *et al.*, 2004).

One of the candidates for m/z 157.1, 4-methylene-L-glutamine has been associated with C5-branched dibasic acid metabolism in three *Saccharomyces* species (*S. paradoxus*, *S. mikatae*, and *S. bayanus*) (KEGG database – <http://www.genome.jp/kegg/>) and is possibly excreted in this case. *MEP3* along with *MEP1* and *MEP2*, all encode ammonium permeases that scavenge ammonium from the medium for use as a nitrogen source (Marini *et al.*, 1997). These genes are expressed when low ammonium concentrations are present in the growth medium, but are repressed at high concentrations of a

good nitrogen source (>20 mM ammonium). Mep3p, which displays the lowest affinity of the three, is most sensitive to lowering of the ammonium concentration below 1 mM (Marini *et al.*, 1997). There is also evidence that fungal Mep proteins mediate diffusion of the uncharged ammonia species across the cytoplasmic membrane (Soupene *et al.*, 2001), and that Mep3p participates in colony morphogenesis (Minarikova *et al.*, 2001). Given the above, it is difficult to pinpoint the exact metabolites excreted under the current experimental setup. However, it is very likely that the peaks contributing to the discrimination are associated with metabolites that directly reflect the deletion of the respective genes.

In summary, desorption ionisation on porous silicon offers considerable promise for rapid metabolic analysis, such as in the metabolic footprinting demonstrated here, enabling rapid screening of mutants prior to more elaborate analyses and perhaps for the detection of transient cellular processes that may go unnoticed under more elaborate sample preparation conditions when the number of samples that are acquired may be limited. The evaluation of the technique for such applications is a subject of future investigations.

Acknowledgements

This work was supported by grants from the BBSRC to RG, DBK and SGO.

References

- Allen, J., Davey, H.M., Broadhurst, D., Heald, J.K., Rowland, J.J., Oliver, S.G. and Kell, D.B. (2003). High-throughput classification of yeast mutants for functional genomics using metabolic footprinting. *Nat. Biotechnol.* **21**, 692–696.
- Allen, J., Davey, H.M., Broadhurst, D., Rowland, J.J., Oliver, S.G. and Kell, D.B. (2004). Discrimination of modes of action of antifungal substances by use of metabolic footprinting. *Appl. Environ. Microbiol.* **70**, 6157–6165.
- Bader, G.D., Heilbut, A., Andrews, B., Tyers, M., Hughes, T. and Boone, C. (2003). Functional genomics and proteomics: charting a multidimensional map of the yeast cell. *Trends Cell Biol.* **13**, 344–356.
- Beck, T. and Hall, M.N. (1999). The TOR signalling pathway controls nuclear localization of nutrient-regulated transcription factors. *Nature* **402**, 689–692.
- Cardenas, M.E., Cutler, N.S., Lorenz, M.C., Di Como, C.J. and Heitman, J. (1999). The TOR signaling cascade regulates gene expression in response to nutrients. *Genes Dev.* **13**, 3271–3279.
- Castrillo, J.I. and Oliver, S.G. (in press) Metabolomics and systems biology in *Saccharomyces cerevisiae* in K. E. (Ed), *Fungal Genomics*. Springer Verlag.
- Cooper, T.G. (2002). Transmitting the signal of excess nitrogen in *Saccharomyces cerevisiae* from the Tor proteins to the GATA factors: connecting the dots. *FEMS Microbiol. Rev.* **26**, 223–238.
- Courchesne, W.E. and Magasanik, B. (1988). Regulation of nitrogen assimilation in *Saccharomyces cerevisiae*: roles of the URE2 and GLN3 genes. *J. Bacteriol.* **170**, 708–713.
- Crespo, J.L., Powers, T., Fowler, B. and Hall, M.N. (2002). The TOR-controlled transcription activators GLN3, RTG1, and RTG3 are regulated in response to intracellular levels of glutamine. *Proc. Natl. Acad. Sci. U.S.A.* **99**, 6784–6789.
- Daran-Lapujade, P., Jansen, M.L., Daran, J.M., van Gulik, W., de Winde, J.H. and Pronk, J.T. (2004). Role of transcriptional regulation in controlling fluxes in central carbon metabolism of *Saccharomyces cerevisiae*. A chemostat culture study. *J. Biol. Chem.* **279**, 9125–9138.
- Daugherty, J.R., Rai, R., el Berry, H.M. and Cooper, T.G. (1993). Regulatory circuit for responses of nitrogen catabolic gene expression to the GLN3 and DAL80 proteins and nitrogen catabolite repression in *Saccharomyces cerevisiae*. *J. Bacteriol.* **175**, 64–73.
- Dunn, W.B., Bailey, N.J.C. and Johnson, H.E. (2005). Measuring the metabolome: current analytical technologies. *Analyst* **130**, 606–625.
- Dunn, W.B. and Ellis, D.I. (2005). Metabolomics: current analytical platforms and methodologies. *Trends Anal. Chem.* **24**, 285–294.
- Go, E.P., Prenni, J.E., Wei, J., Jones, A., Hall, S.C., Witkowska, H.E., Shen, Z. and Siuzdak, G. (2003a). Desorption/ionization on silicon time-of-flight/time-of-flight mass spectrometry. *Anal. Chem.* **75**, 2504–2506.
- Go, E.P., Shen, Z., Harris, K. and Siuzdak, G. (2003b). Quantitative analysis with desorption/ionization on silicon mass spectrometry using electrospray deposition. *Anal. Chem.* **75**, 5475–5479.
- Goodacre, R., Timmins, E.M., Burton, R., Kaderbhai, N., Woodward, A.M., Kell, D.B. and Rooney, P.J. (1998). Rapid identification of urinary tract infection bacteria using hyperspectral whole-organism fingerprinting and artificial neural networks. *Microbiology* **144**(Pt 5), 1157–1170.
- Goodacre, R., Vaidyanathan, S., Dunn, W.B., Harrigan, G.G. and Kell, D.B. (2004). Metabolomics by numbers: acquiring and understanding global metabolite data. *Trends Biotechnol.* **22**, 245–252.
- Ideker, T., Thorsson, V., Ranish, J.A., Christmas, R., Buhler, J., Eng, J.K., Bumgarner, R., Goodlett, D.R., Aebersold, R., Hood, L., (2001). Integrated genomic and proteomic analyses of a systematically perturbed metabolic network. *Science* **292**, 929–934.
- Jones, D.L., Petty, J., Hoyle, D.C., Hayes, A., Ragni, E., Popolo, L., Oliver, S.G. and Stateva, L.I. (2003). Transcriptome profiling of a *Saccharomyces cerevisiae* mutant with a constitutively activated Ras/cAMP pathway. *Physiol. Genomics* **16**, 107–118.
- Kaderbhai, N.N., Broadhurst, D.I., Ellis, D.I., Goodacre, R. and Kell, D.B. (2003). Functional genomics via metabolic footprinting: monitoring metabolite secretion by *Escherichia coli* tryptophan metabolism mutants using FT-IR and direct injection electrospray mass spectrometry. *Comp. Funct. Genomics* **4**, 376–391.
- Kell, D.B., Brown, M., Davey, H.M., Dunn, W.B., Spasic, I. and Oliver, S.G. (in press) Metabolic footprinting and systems biology: the medium is the message. *Nat. Rev. Microbiol.*
- Kuruvilla, F.G., Shamji, A.F. and Schreiber, S.L. (2001). Carbon- and nitrogen-quality signaling to translation are mediated by distinct GATA-type transcription factors. *Proc. Natl. Acad. Sci. U.S.A.* **98**, 7283–7288.
- Magasanik, B. and Kaiser, C.A. (2002). Nitrogen regulation in *Saccharomyces cerevisiae*. *Gene* **290**, 1–18.
- Marini, A.M., Soussi-Boudekou, S., Vissers, S. and Andre, B. (1997). A family of ammonium transporters in *Saccharomyces cerevisiae*. *Mol. Cell Biol.* **17**, 4282–4293.
- Minarikova, L., Kuthan, M., Ricicova, M., Forstova, J. and Palkova, Z. (2001). Differentiated gene expression in cells within yeast colonies. *Exp. Cell Res.* **271**, 296–304.
- Mitchell, A.P. and Magasanik, B. (1984). Regulation of glutamine-repressible gene products by the GLN3 function in *Saccharomyces cerevisiae*. *Mol. Cell Biol.* **4**, 2758–2766.

- Oliver, S.G., Winson, M.K., Kell, D.B. and Baganz, F. (1998). Systematic functional analysis of the yeast genome. *Trends Biotechnol.* **16**, 373–378.
- Raamsdonk, L.M., Teusink, B., Broadhurst, D., Zhang, N., Hayes, A., Walsh, M.C., Berden, J.A., Brindle, K.M., Kell, D.B., Rowland, J.J., Westerhoff, H.V., van Dam, K. and Oliver, S.G. (2001). A functional genomics strategy that uses metabolome data to reveal the phenotype of silent mutations. *Nat. Biotechnol.* **19**, 45–50.
- Shen, Z., Thomas, J.J., Averbuj, C., Broo, K.M., Engelhard, M., Crowell, J.E., Finn, M.G. and Siuzdak, G. (2001). Porous silicon as a versatile platform for laser desorption/ionization mass spectrometry. *Anal. Chem.* **73**, 612–619.
- Soupe, E., Ramirez, R.M. and Kustu, S. (2001). Evidence that fungal MEP proteins mediate diffusion of the uncharged species NH₃ across the cytoplasmic membrane. *Mol. Cell Biol.* **21**, 5733–5741.
- ter Kuile, B.H. and Westerhoff, H.V. (2001). Transcriptome meets metabolome: hierarchical and metabolic regulation of the glycolytic pathway. *FEBS Lett.* **500**, 169–171.
- Trauger, S.A., Go, E.P., Shen, Z., Apon, J.V., Compton, B.J., Bouvier, E.S., Finn, M.G. and Siuzdak, G. (2004). High sensitivity and analyte capture with desorption/ionization mass spectrometry on silylated porous silicon. *Anal. Chem.* **76**, 4484–4489.
- Vaidyanathan, S. (2005). Profiling microbial metabolomes: what do we stand to gain?. *Metabolomics* **1**, 17–28.
- Vaidyanathan, S., Harrigan, G.G. and Goodacre, R. (Eds) (2005). *Metabolome Analyses: Strategies for Systems Biology*. Springer, New York.
- Vazquez, A., Flammini, A., Maritan, A. and Vespignani, A. (2003). Global protein function prediction from protein-protein interaction networks. *Nat. Biotechnol.* **21**, 697–700.
- Velasco, I., Tenreiro, S., Calderon, I.L. and Andre, B. (2004). *Saccharomyces cerevisiae* Aqr1 is an internal-membrane transporter involved in excretion of amino acids. *Eukaryot. Cell* **3**, 1492–1503.
- Wei, J., Buriak, J.M. and Siuzdak, G. (1999). Desorption-ionization mass spectrometry on porous silicon. *Nature* **399**, 243–246.
- Wu, J., Zhang, N., Hayes, A., Panoutsopoulou, K. and Oliver, S.G. (2004). Global analysis of nutrient control of gene expression in *Saccharomyces cerevisiae* during growth and starvation. *Proc. Natl. Acad. Sci. U.S.A.* **101**, 3148–3153.
- Zhu, X., Garrett, J., Schreve, J. and Michaeli, T. (1996). GNP1, the high-affinity glutamine permease of *S. cerevisiae*. *Curr. Genet.* **30**, 107–114.